

Chiral Selectivity in the Binding of [4]Helicene Derivatives to Double-Stranded DNA

Oksana Kel,^[a] Alexandre Fürstenberg,^[b] Nathalie Mehanna,^[c] Cyril Nicolas,^[c] Benoît Laleu,^[c] Martin Hammarskjöld,^[d] Bo Albinsson,^[d] Jérôme Lacour,^[c] and Eric Vauthey*^[a]

Abstract: The interaction of a series of chiral cationic [4]helicene derivatives, which differ by their substituents, with double-stranded DNA has been investigated by using a combination of spectroscopic techniques, including time-resolved fluorescence, fluorescence anisotropy, and linear dichroism. Addition of DNA to helicene solutions results to a hypochromic shift of the visible absorption bands, an increase of fluores-

cence quantum yield and lifetime, a slowing down of fluorescence anisotropy decay, and a linear dichroism in flow-oriented DNA, which unambiguously points to the binding of these

Keywords: chirality • circular dichroism • DNA recognition • fluorescent probes • helical structures • time-resolved spectroscopy

dyes to DNA. Both helicene monomers and dimeric aggregates, which form at higher concentration, bind to DNA, the former most probably upon intercalation and the latter upon groove binding. The binding constant depends substantially on the dye substituents and is, in all cases, larger with the *M* than the *P* enantiomer, by factors ranging from 1.2 to 2.3, depending on the dye.

Introduction

Chirality is of paramount importance for numerous processes in biological systems. It is intrinsically present in the structure of DNA, both at the molecular and supramolecular levels, and plays a crucial role in the functionality of DNA because it guides its interaction with other chemical species, such as enzymes or drugs. Gaining a deeper insight into the molecular mechanisms involved in these specific interactions is very challenging. The synthesis of the unnatural enantiomers of biological macromolecules is a major difficulty. One way to overcome this complication is to study the interaction of DNA with small chiral organic molecules that

are easier to access.^[1] Moreover, molecules that are able to bind strongly and specifically to DNA can be potentially used in therapeutical applications,^[2] medical diagnostics,^[3] and genetic screenings.^[4]

Over the last decades, the interaction between numerous drugs and different DNA sequences and conformations has been intensively studied. Several chiral dyes have been reported to exhibit stereoselectivity for DNA. For example, the anticancer drug daunorubicin,^[5] which exists naturally as the *P* enantiomer, and its synthetic *M* stereoisomer (WP900) clearly show distinct behaviours with B- and Z-DNA,^[6] the *P* and *M* forms binding selectively to the right-handed B- and left-handed Z-DNA, respectively. Planar polycyclic aromatic hydrocarbons that usually bind efficiently to DNA can be made chiral upon addition of specific substituents. For example, the *S* enantiomers of piperazinecarbonyloxyalkyl derivatives of anthracene and pyrene have been shown to preferentially bind to B-DNA.^[7] Numerous monomeric and linked polyamides have been used to elucidate the influence of chirality on binding ability.^[8] For this group of molecules, the binding affinity to B-DNA of the *R* enantiomer is, in general, strongly enhanced. Other molecules that belong to the helicene family have also been used to examine chiral selectivity.^[9] For example, the *P* enantiomer of helicene, bearing a protonated amino group, displays structural selectivity for binding to DNA as it discriminates between B- and Z-DNA.^[10] In the latter case, the binding mode was not determined.

Due to the high importance of DNA-metal interactions, a vast number of organometallic complexes have been investigated in nucleic acid environments.^[1b,11] It has been shown that the enantioselectivity of DNA binding and the appear-

[a] Dr. O. Kel, Prof. E. Vauthey
Department of Physical Chemistry, University of Geneva
30, quai Ernest-Ansermet, 1211 Genève 4 (Switzerland)
E-mail: eric.vauthey@unige.ch

[b] Dr. A. Fürstenberg
Department of Human Protein Sciences, University of Geneva
CMU, Rue Michel-Servet 1, 1211 Genève 4 (Switzerland)

[c] Dr. N. Mehanna, Dr. C. Nicolas, Dr. B. Laleu, Prof. J. Lacour
Department of Organic Chemistry, University of Geneva
30, quai Ernest-Ansermet, 1211 Genève 4 (Switzerland)

[d] M. Hammarskjöld, Prof. B. Albinsson
Department of Chemical and
Biological Engineering/Physical Chemistry
Chalmers University of Technology
41296 Gothenburg (Sweden)

 Supporting information for this article is available on the WWW under <http://dx.doi.org/10.1002/chem.201203915>.

ance of undesired effects such as toxicity or mutagenicity strongly depend on the chirality of these complexes. For example, the *R,R* isomer of platinum complexes with 1,2-diaminocyclohexane and other ligands are less toxic and more efficient anticancer drugs than the *S,S* isomer.^[12] Similarly, chiral selectivity of numerous other metal complexes with iron, rhodium, ruthenium and osmium has been used as a tool for probing different DNA conformations.^[13]

In general, molecules interacting with DNA can be split into two main groups: those that intercalate and those that bind to the minor or major grooves of DNA.^[14] In the first case, the dye is inserted between two base pairs in the double helix with its molecular plane parallel to that of the neighbouring base pairs. Because the distance between DNA base pairs is small, intercalation occurs mostly with small planar aromatic molecules. Moreover, it very often induces a lengthening and unwinding of the DNA helix. Furthermore, the base pairs can be tilted by several degrees compared with their usual arrangement (perpendicular to the long DNA axis) upon dye intercalation.

The variety of groove-binding molecules is much broader and includes molecules with different structures. Because of the size of the grooves, groove binding results in a smaller distortion of the DNA duplex structure than intercalation. It is often presumed that small molecules interact with the minor groove, whereas large dyes tend, for steric reasons, to bind to the major groove.^[16] The binding to the minor groove is stabilised by the strong electronegative potential of the AT base pairs.^[15] Alternatively, the amino group of guanine in GC base pairs generates a steric barrier for binding to the minor groove.

The cationic [4]helicene derivatives (HelR) depicted in Figure 1 represent new, intrinsically chiral aromatic dyes.

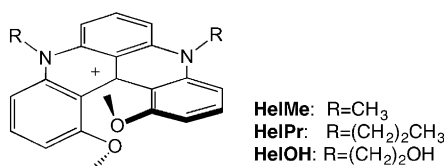


Figure 1. (*M*)-HelR dyes.

emitting in the NIR region.^[16] Due to their favourable properties, namely their aromatic and positively charged structure, HelR can be used for exploring recognition mechanisms in biological systems. We report here on a detailed investigation of the interaction of different enantiopure forms of HelR with right-handed double stranded DNA (dsDNA). Evidence for binding is provided by different techniques including stationary and time-resolved absorption and fluorescence spectroscopy. Furthermore, linear dichroism spectroscopy was used to establish the binding mode. The influence of the substituents on the binding ability, binding geometry and chiral selectivity will be discussed.

Results

Steady-state experiments: The absorption spectra of the HelR dyes in aqueous solution exhibit three major bands between $\lambda = 300$ and 700 nm, with maxima that depend only slightly on the R substituents (Figure 2A).^[17] Significant

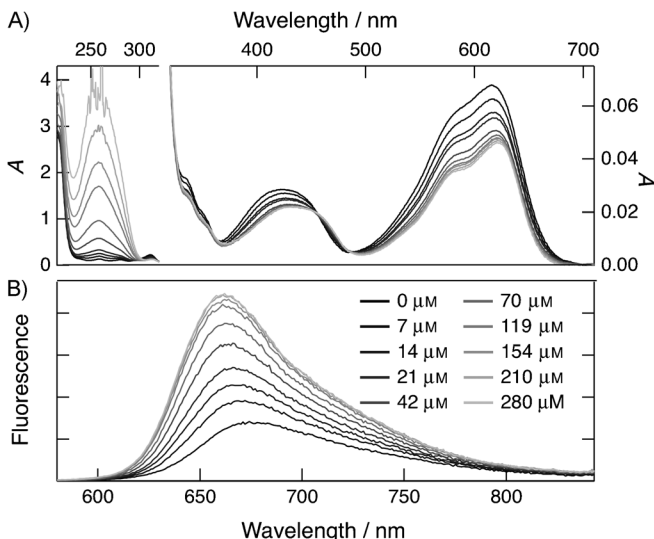


Figure 2. A) Absorption and B) fluorescence spectra measured with a $5 \mu\text{M}$ aqueous solution of *(P)*-HelPr and different concentrations of ssDNA base pairs.

changes in the absorption spectra arise upon addition of double-stranded salmon sperm DNA (sspDNA): the intensity of all three bands decreases, their maxima undergo a small redshift and their shapes change, with the shoulder around 580 nm becoming more pronounced, the band around 430 nm broader, and that around 615 nm narrower. These effects were observed with all HelR samples, irrespective of whether they were racemic mixtures or enantiopure. Simultaneously to these changes, significant alterations of the fluorescence spectrum appear upon addition of sspDNA (Figure 2B): the emission band narrows, shifts to shorter wavelengths and its intensity increases. At a given DNA concentration, the band intensity stops rising, indicating that all HelR present in solution are bound to DNA. The fluorescence quantum yields, Φ_{fl} , determined for the free and DNA-bound HelR are listed in Table 1. Upon binding to DNA, the fluorescence of the HelR dyes increases by factors varying between 3.1 and 4.4, depending on R and the chirality of the dye.

As previously discussed in detail,^[17] the HeLR dyes tend to form dimeric aggregates in aqueous solutions. Therefore, all DNA titration experiments were performed at very low HeLR concentration (1–6 μ M) to minimize dimerization. The relative concentrations of free and DNA-bound HeLR dyes were determined from the absorption spectra by assuming that all dyes are in monomeric form at the beginning of the titration and bound to DNA after saturation of the fluores-

Table 1. Fluorescence quantum yields of free and DNA-bound HelR dyes.

HelR	Φ_{fl} (free)	Φ_{fl} (bound)	Contrast
(<i>M</i>)-HelMe	0.014	0.061	4.4
(<i>P</i>)-HelMe	0.018	0.064	3.5
(<i>rac</i>)-HelMe	0.019	0.083	4.4
(<i>M</i>)-HelPr	0.026	0.095	3.7
(<i>P</i>)-HelPr	0.026	0.088	3.4
(<i>rac</i>)-HelPr	0.026	0.10	3.8
(<i>M</i>)-HelOH	0.016	0.06	3.7
(<i>P</i>)-HelOH	0.016	0.05	3.1
(<i>rac</i>)-HelOH	0.016	0.06	3.7

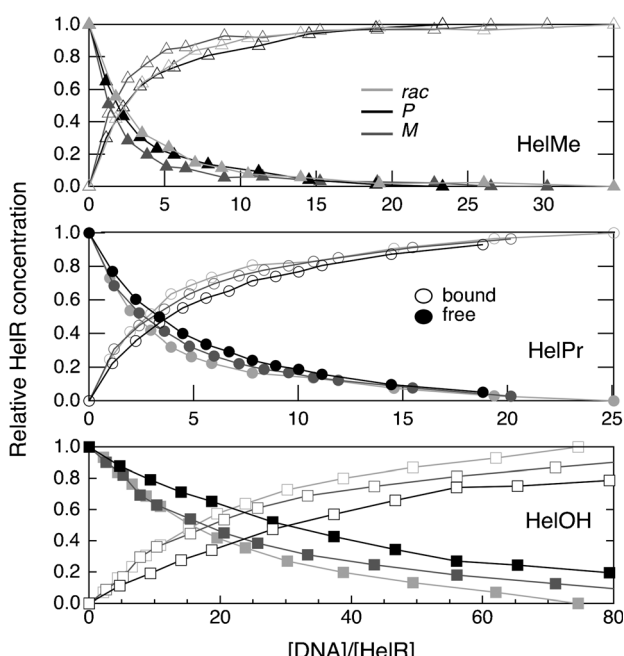


Figure 3. Relative concentrations of free and DNA-bound HelR dyes as a function of sspDNA base-pair concentration determined from the absorption spectra. Open symbols denote bound and filled symbols free dye, respectively.

cence signal. The decrease of the relative concentration of free HelR dyes upon addition of DNA is depicted in Figure 3.

The interaction of HelR dyes with DNA can also be detected from circular and linear dichroism measurements. The circular dichroism (CD) spectra of the dyes change upon addition of sspDNA because of the coupling of the electric transition dipoles of the HelR with those of the nucleobases (Figure 4). The bands are slightly redshifted and the rotational strength of the positive bands increases (except for the $\lambda=615$ nm band), whereas that of the negative bands become smaller. In the UV region, the sspDNA bands overlap with those of the dyes.

As shown in Figure S1, the intensity of the CD signals decrease linearly with decreasing HelR concentration, whereas the shape of the spectra is unaltered.

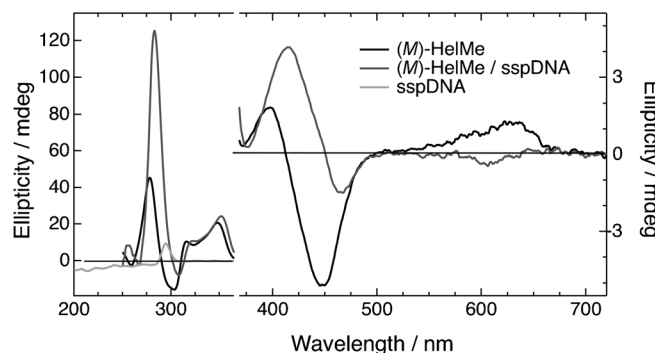


Figure 4. CD spectra of an aqueous solution of (*M*)-HelMe (17 μ M) with and without sspDNA, and of a solution of sspDNA (0.65 μ M).

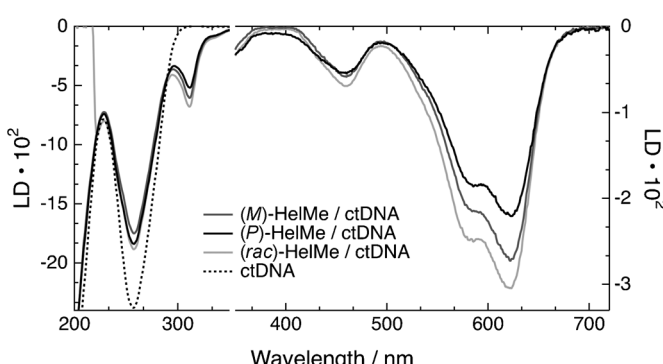


Figure 5. LD spectra measured with an aqueous solution of ctDNA (60 μ M) and with racemic and enantiopure HelMe ($[(M\text{-})\text{HelMe}]=45$ μ M; $[(P\text{-})\text{HelMe}]=56$ μ M; $[(rac\text{-})\text{HelMe}]=86$ μ M).

Figure 5 shows linear dichroism (LD) spectra of flow-oriented racemic and enantiopure HelMe with calf-thymus DNA (ctDNA). The existence of an LD signal confirms the interaction of the dyes with DNA. Indeed, noninteracting dyes have a random orientation relative to the ctDNA strands and, thus, do not exhibit any dichroism. For HelMe and all the HelR investigated, the LD spectra consist of three negative bands around $\lambda=615$, 460 and 310 nm, originating from HelR, and a very intense peak at 257 nm arising from ctDNA. Figure 6 shows that an increase in the HelR concentration leads to changes in the intensity and shape of the LD spectra. The 580 nm shoulder becomes more pronounced and the intensity around 400 nm decreases (Figure 6B).

Time-resolved fluorescence measurements: For time-correlated single photon-counting (TCSPC) measurements, much higher dye concentrations (20–30 μ M) than for the steady-state experiments described so far had to be used. As previously discussed in detail,^[17] the fluorescence decays measured with aqueous HelR solutions in this concentration range are biexponential with 1–2 and 4–5 ns time constants due to the emission of the monomeric and dimeric forms, respectively. Upon addition of sspDNA, the fluorescence decays measured with the HelR enantiomers and racemic

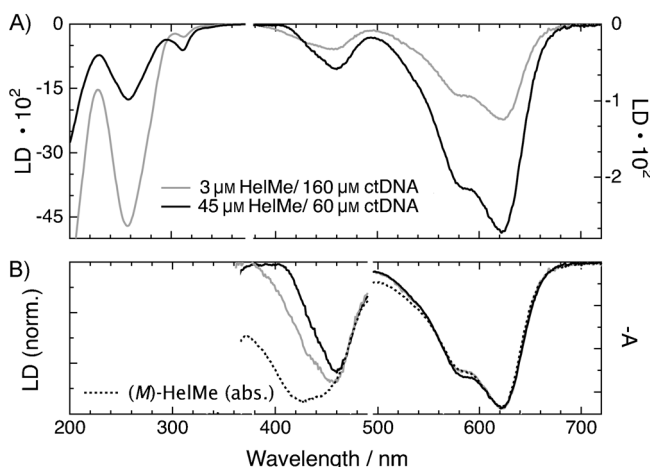


Figure 6. A) LD spectra of flow oriented solutions of ctDNA with different (M)-HelMe concentrations and B) comparison of the intensity normalised LD spectra with the absorption spectrum of (M)-HelMe in water.

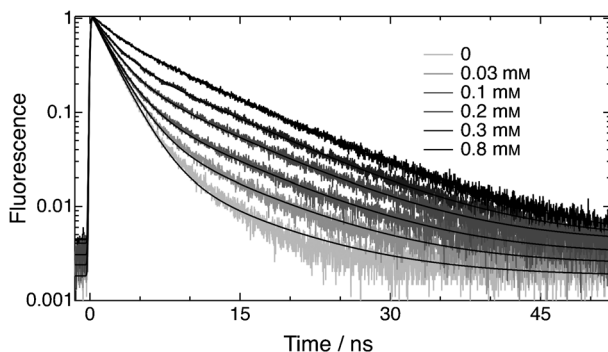


Figure 7. Intensity-normalised fluorescence decays measured with (M)-HelPr and increasing concentrations of sspDNA. The black lines indicate the result of a global biexponential analysis.

mixtures slow down significantly, as illustrated in Figure 7. Each individual decay measured with a given HelR and sspDNA concentration could be very well reproduced with a biexponential function. However, the decays measured with different sspDNA concentrations could only be partially reproduced when performing a global biexponential analysis (Figure 7). The shorter time constant was found to be of the order of 1.3–2 ns, that is, close to that measured for the decay of the monomeric emission, whereas the longer was between 5 and 8 ns (Table S1). As discussed below, both HelR monomer and dimer probably bind to DNA, and thus four fluorescent species should be present in solution and a four-exponential decay should be expected. However, the fluorescence lifetimes of each of the four species cannot be reliably distinguished. Whereas the monomer is responsible for the short decay component, the other three forms, namely the DNA-bound monomer and the free and DNA-bound dimers, probably have similar lifetimes and contribute to the long decay component of the fluorescence.

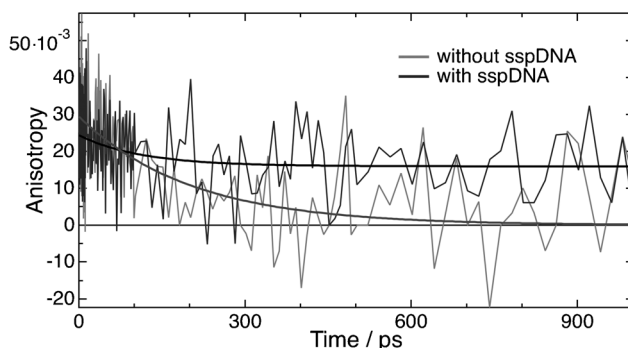


Figure 8. Fluorescence anisotropy decay measured with (M)-HelMe with and without sspDNA and best single exponential fits.

Even higher HelR concentrations (90–100 μM) had to be used for the time-resolved fluorescence anisotropy measurements, although the HelR/sspDNA ratio was kept at 1/60. Figure 8 depicts the fluorescence anisotropy decay measured with (M)-HelMe with and without sspDNA after 400 nm excitation. The poor signal to noise ratio originates from the very small (0.025–0.03) initial anisotropy at this wavelength.^[17] A monoexponential function with a lifetime of (200±50) ps can reproduce the anisotropy decay of (M)-HelMe in aqueous solution, whereas in the presence of DNA, at least two exponential functions are needed. In the latter case, the first time constant around (110±30) ps can be ascribed to diffusional reorientation of the free dye in solution. The second time constant is much longer (more than 10 ns) than our time window and cannot be determined precisely. It can be attributed to the slow tumbling of the DNA-bound HelR.

Discussion

Evidence of binding: The large changes in the absorption, fluorescence and CD spectra observed with the HelR dyes upon addition of DNA (Figure 2 and Figure 4), together with the increase of fluorescence quantum yield and lifetime (Figure 7) unambiguously point to binding of the HelR dyes to DNA. The LD signal recorded with the dyes in solution in the presence of oriented DNA is further clear evidence of their interaction, as is the significant slowing down of the fluorescence anisotropy decay upon addition of DNA. A similar slowing down has been reported for other dyes upon binding to biological macromolecules.^[18]

The decrease of the extinction coefficient of the HelR dyes upon binding to DNA (Figure 2A) points to a significant decrease of their radiative rate constant, k_r . Unfortunately, the k_r value of the DNA-bound dyes cannot be directly calculated from the fluorescence decay, because four fluorescent species (monomer and dimer HelR, both either free or bound to DNA), three of which have very similar fluorescence lifetimes, contribute to the total decay. In a previous work, it has been shown that the radiative rate constant of the HelR dye is not very sensitive to the environ-

ment and is almost solvent independent.^[17] Consequently, the observed hypochromism and the ensuing decrease of k_t probably arise from some structural alteration of the dyes upon binding to DNA or some electronic coupling with the DNA bases. Such hypochromism upon DNA binding has already been reported with other dyes binding to DNA upon intercalation.^[19] On the other hand, both the fluorescence lifetime and quantum yield of the HelR dyes have been shown to increase by a factor of 3–4 by going from aqueous solutions to organic solvents.^[17] As a consequence, the increase of fluorescence lifetime and quantum yield measured here upon addition of DNA could be accounted for by the intercalation of the HelR dyes into DNA and a reduced exposure to water.

It is important to note that the shape of the LD spectra depends on the DNA/dye ratio (Figure 6B). These differences can arise from either 1) the existence of two different DNA-binding modes of the monomeric dyes or 2) the ability of the HelR dimers to bind to DNA as well. The appearance in the LD spectra of the $\lambda=580$ nm shoulder (the main feature of HelR dimers)^[17] speaks in favour of interaction of the dimers with DNA. Thus, both HelR monomers and dimers bind to DNA and the experimentally observed LD signal consists of at least two contributions. However, it is not clear whether the dimers bind to DNA directly or whether dimerisation takes place between a free monomer and another one already bound to DNA.

In contrast to other molecules that have several DNA binding modes,^[20] no changes in the CD spectra with increasing HelR concentration were observed (Figure S1). This lack of changes can be explained by very similar CD spectra of monomer and dimer bound to DNA, which are consequently almost indistinguishable. Another possibility might be that the range of concentration chosen is not sufficiently broad.

Binding geometry: Analysis of the sign and relative amplitude of the LD signal provides information about the orientation of the bound molecules.^[15] Figure 9 shows the reduced linear dichroism (LD^r) spectra recorded with very low HelR concentration to minimize the signal originating from bound dimers. The LD^r amplitudes of the HelR bands are more negative than that of the DNA band at $\lambda=260$ nm. The same effect was previously observed with other molecules that are known to intercalate into DNA, for example oxazole yellow (YO) cyanines,^[19a] ruthenium polypyridyl complexes,^[21] phenothiazinium,^[22] and acridine dyes.^[23] Two possible explanations can be suggested: first, dye intercalation can tilt the DNA bases, and, second, the DNA may become stiffer at the binding sites and thus better oriented in the flow.

The significant variation in the LD^r amplitude of the DNA band upon addition of HelR (Figure 9) is further evidence of the changes in DNA flow orientation upon interaction with HelR, as mentioned above. As both HelR and DNA absorb in this region, it may also partly originate from an excitonic coupling between the DNA-bases and HelR.

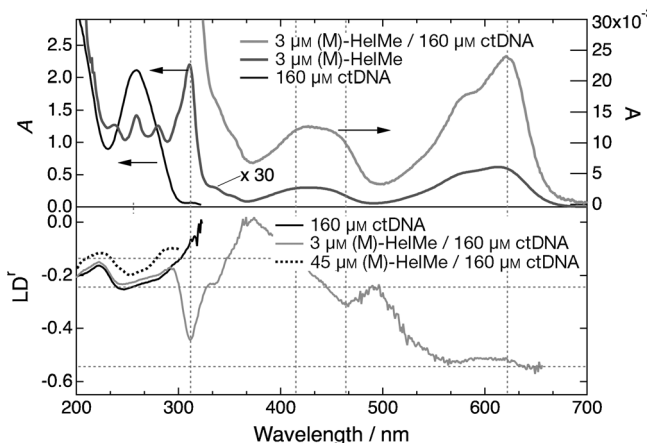


Figure 9. Absorption spectrum of (M)-HelMe and ctDNA and reduced linear dichroism spectra of (M)-HelMe with and without ctDNA. The reduced linear dichroism of the ctDNA band in the presence of a high (M)-HelMe concentration is also shown.

As a result, the LD^r signal of the DNA band cannot be directly used for the determination of the orientational parameter S .

According to time-dependent density functional theory (TD-DFT) calculations performed on the HelR dyes and reported by Kel et al.,^[17] the transition dipole moment associated with the 615 nm band, $\vec{\mu}_1$, is parallel to the y axis (Figure 10 and Figure S2 in the Supporting Information).

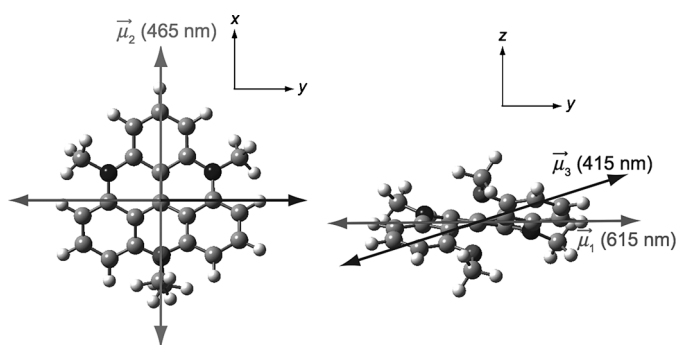


Figure 10. Orientation of the transition dipole moments of HelMe according to TD-DFT calculations described by Kel et al.^[17] The Cartesian coordinates xyz have been chosen so that the transition dipole moments $\vec{\mu}_2$ and $\vec{\mu}_1$ coincide with the x and y axes, respectively.

On the other hand, the band around 430 nm arises from two transitions, that with the lowest energy having its dipole moment, $\vec{\mu}_2$, along the x axis and the other, $\vec{\mu}_3$, located in the yz plane and making an angle of about 30° with $\vec{\mu}_1$. These data, together with the measured LD^r values, were used to estimate the angles between the transition dipole moments and the orientational axis, α_{1-3} . These calculations, described in detail in the Supporting Information, yield $\alpha_1=89$, $\alpha_2=69$ and $\alpha_3=60$ °. These angles suggest that the molecular plane of the HelR dyes is mostly perpendicular to the orientational axis. In other words, the bound HelR dyes

have their molecular plane essentially parallel to the DNA bases, pointing to intercalation rather than groove binding. In the latter case, the molecular plane is expected to be parallel to the orientational axis. These angles should, nevertheless, be considered with some caution because of the possible contribution of dimeric HelR dyes to the LD spectra, the fact that the LD^r values are treated as coming from non-overlapping transitions, which is not the case for those responsible for the 430 nm band, and finally that they are based on calculated transition dipole moments. Nevertheless, Figure 11 and Figure S4 in the Supporting Information

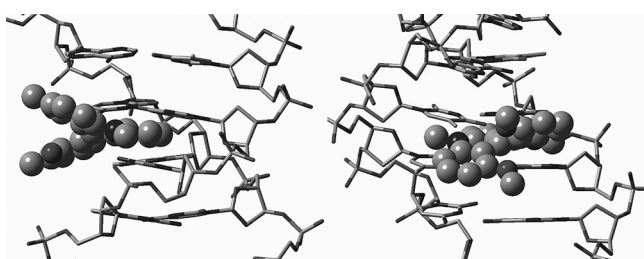


Figure 11. Side (left) and backward (right) views of a hypothetical, non-optimised structure of the HelMe/DNA complex.

show that a HelMe molecule can indeed partially intercalate between DNA base pairs without clear steric hindrance. This hypothetical structure was obtained by manually inserting the gas-phase optimised structure of HelMe into the crystal structure of a d(CGCGAATTCTCGCG)₂ DNA strand obtained from the protein data bank (1BNA.pdb), without further optimisation. Intercalation is further supported by the hypochromism of the HelR absorption band upon interaction with DNA, and by the larger LD^r amplitude of the HelR band compared with the DNA band.^[24] On the other hand, intercalation can be safely excluded for the HelR dimers for steric reasons. This indicates that the free dimers interact directly with DNA and undergo groove binding. Therefore, dimerisation does not occur between a free HelR molecule and a DNA-bound monomer.

Chiral selectivity: The affinity of the HelR dyes for double-stranded DNA can be quantified by the binding constant *K* for the following equilibrium:



The data presented in Figure 3 were analysed using the McGhee and von Hippel model [Eq. (2)].^[25] The best fits of Equation (2) to the dependence of *r*/[HelR] on *r* are shown in Figure S3 and the so-obtained binding constants, *K*, together with the number of base pairs perturbed by a bound dye, *n*, are listed in Table 2.

The binding constants reveal that the HelR dyes exhibit some stereoselectivity in their interaction with DNA. For all dyes investigated, the *M* enantiomer interacts more efficiently with DNA than the *P* enantiomer. This selectivity

Table 2. DNA binding constants (*K*) and number of base pairs involved in the binding (*n*) for the HelR enantiomers determined by using Equation (2).

HelR	<i>n</i>	<i>K</i> [$\times 10^4$]
(<i>M</i>)-HelMe	1.6 \pm 0.2	37 \pm 3
(<i>P</i>)-HelMe	1.7 \pm 0.1	16.2 \pm 4
(<i>M</i>)-HelPr	1.7 \pm 0.1	10.8 \pm 6
(<i>P</i>)-HelPr	1.9 \pm 0.3	8.5 \pm 0.8
(<i>M</i>)-HelOH	1.6 \pm 0.2	3.3 \pm 0.2
(<i>P</i>)-HelOH	1.7 \pm 0.1	2.8 \pm 0.2

originates from the chirality of DNA, which, in its B form, is right-handed. Such preferential binding of the *M* form to DNA has also been observed with other chiral molecules.^[26] The better affinity of the *M* enantiomer of the HelR dyes to DNA is compatible to our proposed intercalation hypothesis. As shown in Figure 11, only the planar part of the dye, consisting of the benzene ring with the two heterocycles, can be expected to intercalate between the DNA base pairs, whereas the two out-of-plane methoxy-benzene rings stick out in the major groove. For the *M* form, these two rings point away from the helical base-pair stack, whereas for the *P* form, they point towards it. Therefore, the *M* form should experience less steric hindrance upon intercalation than the *P* form.

As shown in Table 2, the binding ability of the HelR dyes depends on the nature of the R substituent on the N atoms. The binding constant is highest with methyl substituents, slightly smaller with propyl groups, and significantly smaller with R = (CH₂)₂-OH, although the latter substituent has a similar size to a propyl group. Such difference might be explained by the dissimilar polarity of the two groups. Indeed, intercalation might be favoured with HelPr because it minimizes the exposure of the hydrophobic propyl groups to water. With HelOH, on the other hand, intercalation might lead to a loss of the solvation energy associated with H-bonding between the OH groups and water molecules.

Figure 3 shows that, at a given concentration, the binding affinity measured with the racemic HelR mixtures is not the average of those of the enantiomeric (*M*)- and (*P*)-HelR forms. For HelPr and HelOH, binding with the racemic mixtures is stronger than with the enantiopure compounds. This effect could be explained by a higher binding constant of the dimers, which are present at higher concentrations in the racemic mixtures,^[17] compared with the monomers. The opposite behaviour can be observed with HelMe, pointing to a larger binding constant of the monomer. However, an exact determination of the binding constants of the dimers is complicated by the overlap of the spectral bands and has consequently not been carried out. The same effect is probably at the origin of the similar fluorescence contrasts measured with the (*rac*)- and (*M*)-HelR forms. Therefore, comparison of the fluorescence contrasts is only meaningful with the enantiopure forms, for which the dimerisation constants are the same.

Compared with other molecules that bind to DNA, the HelR dyes have quite good affinity to DNA, their binding

constant being almost one order of magnitude higher than those reported for 2,2,2-trifluoro-1-(9-anthryl)ethanol,^[27] piperazinecarbonyloxy-2-propyl derivatives,^[7] the anticancer drug Daunorubicin,^[6] 5,8-bis(aminomethyl)-1,12-dimethylbenzo[c]phenanthrene,^[9a] and other compounds.^[1b,11a] However, it cannot compete with the strongest binding molecules such as Hoechst 33258,^[8f] and Dervan's polyamides.^[8b,e] On the other hand, the enantioselectivity of the HeLR dyes to DNA ($K_M/K_P \approx 1.5$) is rather small in comparison with other chiral binding probes, such as the hairpin polyamide-Hoechst 33258 conjugate, the *R* enantiomer of which exhibits a 10 to 30 fold high binding affinity than the *S* enantiomer.^[8f] However, contrary to the HeLR studied here, this large enantioselectivity does not originate from the fluorophore itself but rather from the chiral polyamide ligand.

Conclusion

All the various spectroscopic techniques used in this work point unambiguously to binding of the HeLR dyes to DNA. This can be clearly seen by changes in the electronic absorption, CD and fluorescence spectra, by an increasing fluorescence quantum yield and by a slowing down of the fluorescence anisotropy decay. The substituents on the nitrogen atoms strongly affect the binding ability of the dye, the highest binding constant being found with HeLM, which is the smallest hydrophobic substituent. The marked difference between the binding constants of HeLPr and HeLOH shows that the size of the substituents is not the only important factor. The hydroxyl group in HeLOH lowers the binding ability by almost one order of magnitude in comparison with the propyl group. For all three HeLR dyes, the highest binding constant is found with the *M* enantiomer, revealing a clear, but not dramatic, stereoselectivity. Intercalation is the most probable binding mode of the HeLR monomers, whereas the dimers undergo groove binding. One interesting feature of the HeLR dyes is their increasing fluorescence quantum yield upon DNA binding, making the dye-DNA complexes more visible in fluorescence-based techniques. This, together with a near-infrared emission, makes these HeLR dyes promising candidates for biochemical sensing.

Experimental Section

Samples: All racemic HeLR dyes were synthesised according to literature procedures.^[16a,28] Enantiopure HeLM, HeLPr and HeLOH have been described previously.^[16b,c,g,17] Dimethylsulfoxide (DMSO) was purchased from Fluka, phosphate buffer saline (PBS: NaCl 137 mM, KCl 2.8 mM, Na₂HPO₄ 8.1 mM, KH₂PO₄ 1.5 mM), double-stranded salmon sperm DNA (ssDNA) and calf-thymus DNA (ctDNA) were from Sigma-Aldrich. All compounds were of the highest commercially available grade and used as received. Stock solutions of the dyes were prepared in DMSO before every experiment. DNA (1 mg mL⁻¹) stock solutions were stored at -20°C. For steady-state and linear dichroism measurements, the dyes were diluted in 5 mM NaCl buffer, whereas for time-correlated single-photon counting and up-conversion measurements, the dyes were diluted in PBS/EDTA buffer (1 mM of EDTA). ssDNA was used for all experi-

ments except linear dichroism spectroscopy. In the latter case, ctDNA was used because it orients better in the flow.

Steady-state measurements: Absorption spectra were recorded with a Cary 50 spectrophotometer, whereas fluorescence emission and excitation spectra were measured with a Cary Eclipse fluorimeter. All fluorescence spectra were corrected for the wavelength-dependent sensitivity of the detection. The fluorescence quantum yields were determined relative to oxazine 1 perchlorate in ethanol ($\Phi_F = 0.11$).^[29] All CD spectra were measured with a Jasco J-815 spectropolarimeter in a 10 mm cuvette that does not change the polarization of light at RT. All spectra are an average of at least eight scans.

In the DNA titration experiments, the absorption spectra of HeLR were corrected for dilution. The concentrations of free and bound forms were calculated from the absorption spectrum using that of HeLR without DNA (assuming that only free HeLR is present in solution) and that of HeLR at high DNA concentration (assuming that all HeLR are bound). The binding constant K and the parameter n were calculated by using the excluded site model of McGhee and von Hippel [Eq. (2)]:^[25]

$$\frac{r}{[\text{HeLR}]} = K(1 - nr) \left(\frac{1 - nr}{1 - (n - 1)r} \right)^{n-1} \quad (2)$$

in which $r = [\text{HeLR-DNA}]/[\text{HeLR}]$ is the ratio of bound to free dye concentrations. The parameter n represents the number of DNA base pairs that are occluded by a bound dye due to occupation and/or structural perturbation.^[25] Only the data with 15 to 80% of bound HeLR was used in the analysis.^[19b]

LD spectroscopy: LD spectra were measured with a Chirascan LD spectropolarimeter. A homemade outer-rotating quartz Couette flow cell with 1 mm pathlength and a shear flow gradient of 3000 s⁻¹ was used for orienting the samples.^[15,30] All spectra were baseline corrected by subtraction of the spectra recorded without rotation and the LD values corrected to 1 cm pathlength.

The sign and relative amplitude of the measured LD can be used to unravel the binding geometry in terms of angles between the transition dipole moments of the dye and the direction of macroscopic orientation of the sample.^[15] The LD is defined as the difference in absorption of light linearly polarized parallel and perpendicular to the axis of orientation [Eq. (3)]:

$$\text{LD} = A_{\parallel} - A_{\perp} \quad (3)$$

For the determination of the dye orientation, the so-called reduced linear dichroism, LD^r, which is normalized to the absorption of the isotropic sample (A_{iso}), is used [Eq. (4)]. This LD^r value is independent of the dye concentration, pathlength and dipole strength, and depends only on the angle α between the transition dipole moment of the dye and the orientational axis:^[15]

$$\text{LD}^r = \frac{\text{LD}}{A_{iso}} = \frac{3}{2} S(3 \cos^2 \alpha - 1) \quad (4)$$

in which S is an orientational parameter that takes into account the average distribution of angles between the local orientation and the macroscopic orientation direction. For DNA, S can be determined from the LD^r value of the $\pi\pi^*$ transition of the DNA bases at 260 nm as it is commonly accepted that the bases are oriented at 86° relative to the helix (orientational) axis.^[31] The different types of DNA have distinct orientation parameters, because S strongly depends on their length and stiffness.

Time-resolved fluorescence: Fluorescence lifetime measurements on the nanosecond timescale were performed by using the TCSPC set-up described in detail elsewhere.^[32] Excitation was carried out at 395 nm with a laser diode (Picoquant model LDH-P-C-400B) generating ca. 60 ps pulses at 10 MHz. The instrument response function (IRF) had a full-width at half-maximum (FWHM) of about 200 ps.

The excited-state dynamics of the HeLR dyes was additionally measured by fluorescence up-conversion (FU).^[33] Excitation was achieved at 400 nm with the frequency-doubled output of a Kerr lens mode-locked

Ti:Sapphire laser (Mai Tai, Spectra-Physics). The polarization of the pump pulses was at magic angle relative to that of the gate pulses at 800 nm. For anisotropy measurements, the polarization of the gate pulses at 800 nm was varied with a $\lambda/2$ plate. The pump intensity on the sample was of the order of $5 \mu\text{J cm}^{-2}$ and the FWHM of the IRF was ca. 210 fs. The sample solutions were located in a 0.4 mm thick rotating cell and had an absorbance of ca. 0.1 at 400 nm.

Acknowledgements

This work was supported by the Fonds National Suisse de la Recherche Scientifique, Project Nrs. 200020-124393, 200020-125125, and 200020-135072, the NCCR Chemical Biology and the University of Geneva. Generous funds from the Swedish Research Council (VR) are also acknowledged.

[1] a) H. Ihmels, K. Faulhaber, D. Vedaldi, F. Dall'Acqua, G. Viola, *Photochem. Photobiol.* **2005**, *81*, 1107–1115; b) R. Corradini, S. Sforza, T. Tedeschi, R. Marchelli, *Chirality* **2007**, *19*, 269–294; c) B. A. Neto, A. A. M. Lapis, *Molecules* **2009**, *14*, 1725–1746.

[2] R. Kranaster, A. Marx, *Chem. Eur. J.* **2007**, *13*, 6115–6122.

[3] S. A. E. Marras, S. Tyagi, F. R. Kramer, *Clin. Chim. Acta* **2006**, *363*, 48–60.

[4] S. Werder, V. L. Malinovskii, R. Haner, *Org. Lett.* **2008**, *10*, 2011–2014.

[5] A. H. J. Wang, G. Ughetto, G. J. Quigley, A. Rich, *Biochemistry* **1987**, *26*, 1152–1163.

[6] X. G. Qu, J. O. Trent, I. Fokt, W. Priebe, J. B. Chaires, *Proc. Natl. Acad. Sci. USA* **2000**, *97*, 12032–12037.

[7] H. C. Becker, B. Norden, *J. Am. Chem. Soc.* **2000**, *122*, 8344–8349.

[8] a) M. P. Singh, B. Plouvier, G. C. Hill, J. Gueck, R. T. Pon, J. W. Lown, *J. Am. Chem. Soc.* **1994**, *116*, 7006–7020; b) J. W. Trauger, E. E. Baird, P. B. Dervan, *Nature* **1996**, *382*, 559–561; c) C. L. Kielkopf, S. White, J. W. Szwewczyk, J. M. Turner, E. E. Baird, P. B. Dervan, D. C. Rees, *Science* **1998**, *282*, 111–115; d) D. M. Herman, E. E. Baird, P. B. Dervan, *J. Am. Chem. Soc.* **1998**, *120*, 1382–1391; e) P. B. Dervan, *Bioorg. Med. Chem.* **2001**, *9*, 2215–2235; f) P. M. Reddy, J. W. Toprowski, A. L. Kahane, T. C. Bruice, *Bioorg. Med. Chem. Lett.* **2005**, *15*, 5531–5536.

[9] a) S. Honzawa, H. Okubo, S. Anzai, M. Yamaguchi, K. Tsumoto, I. Kumagai, *Bioorg. Med. Chem.* **2002**, *10*, 3213–3218; b) R. Passeri, A. G. Gaetano, F. Elisei, L. Latterini, T. Caronna, F. Fontana, S. I. Natali, *Photochem. Photobiol. Sci.* **2009**, *8*, 1574–1582.

[10] Y. Xu, Y. X. Zhang, H. Sugiyama, T. Umano, H. Osuga, K. Tanaka, *J. Am. Chem. Soc.* **2004**, *126*, 6566–6567.

[11] a) T. W. Hambley, *Coord. Chem. Rev.* **1997**, *166*, 181–223; b) E. R. Jamieson, S. J. Lippard, *Chem. Rev.* **1999**, *99*, 2467–2498; c) K. E. Erkkila, D. T. Odom, J. K. Barton, *Chem. Rev.* **1999**, *99*, 2777–2795; d) M. Benedetti, J. Malina, J. Kasparkova, V. Brabec, G. Natile, *Environ. Health Perspect.* **2002**, *110*, 779–782.

[12] a) K. Okamoto, M. Noji, T. Tashiro, Y. Kidani, *Chem. Pharm. Bull.* **1981**, *29*, 929–939; b) K. Vickery, A. M. Bonin, R. R. Fenton, S. Omara, M. J. McKeage, P. J. Russell, T. W. Hambley, *J. Med. Chem.* **1993**, *36*, 3663–3668; c) R. R. Fenton, W. J. Easdale, H. M. Er, S. M. Omara, M. J. McKeage, P. J. Russell, T. W. Hambley, *J. Med. Chem.* **1997**, *40*, 1090–1098; d) B. Spangler, D. A. Whittington, S. J. Lippard, *J. Inorg. Biochem.* **2001**, *86*, 440–440; e) J. Malina, J. Kasparkova, G. Natile, V. Brabec, *Chem. Biol.* **2002**, *9*, 629–638.

[13] a) B. Nordén, F. Tjerneld, *FEBS Lett.* **1976**, *67*, 368–370; b) J. K. Barton, L. A. Basile, A. Danishefsky, A. Alexandrescu, *Proc. Natl. Acad. Sci. USA* **1984**, *81*, 1961–1965; c) A. Sitolani, E. C. Long, A. M. Pyle, J. K. Barton, *J. Am. Chem. Soc.* **1992**, *114*, 2303–2312; d) C. L. Kielkopf, K. E. Erkkila, B. P. Hudson, J. K. Barton, D. C. Rees, *Nat. Struct. Biol.* **2000**, *7*, 117–121.

[14] V. A. Bloomfield, D. M. Crothers, I. Tinoco, Jr., *Nucleic Acids: Structures, Properties and Functions*, University Science Books, **2000**, p. 800.

[15] B. Norden, A. Rodgers, T. Dafforn, *Linear Dichroism and Circular Dichroism: A Textbook on Polarized-Light Spectroscopy*, Royal Society of Chemistry, Cambridge, **2010**.

[16] a) B. W. Laursen, F. C. Krebs, *Angew. Chem.* **2000**, *112*, 3574–3576; *Angew. Chem. Int. Ed.* **2000**, *39*, 3432–3434; b) C. Herse, D. Bas, F. C. Krebs, T. Bürgi, J. Weber, T. Wesołowski, B. W. Laursen, J. Lacour, *Angew. Chem. Int. Ed.* **2003**, *42*, 3162; c) B. Laleu, P. Mobian, C. Herse, B. W. Laursen, G. Hopfgartner, G. Bernardinelli, J. Lacour, *Angew. Chem.* **2005**, *117*, 1913–1917; *Angew. Chem. Int. Ed.* **2005**, *44*, 1879–1883; d) C. Villani, B. Laleu, P. Mobian, J. Lacour, *Chirality* **2007**, *19*, 601–606; e) D. Conreaux, N. Mehanna, C. Herse, J. Lacour, *J. Org. Chem.* **2011**, *76*, 2716–2722; f) J. Guin, C. Besnard, P. Pattison, J. Lacour, *Chem. Sci.* **2011**, *2*, 425–428; g) N. Mehanna, S. Grass, J. Lacour, *Chirality* **2012**, *24*, 928–935; h) J. Elm, J. Lykkebo, T. J. Sørensen, B. W. Laursen, K. V. Mikkelsen, *J. Phys. Chem. A* **2011**, *115*, 12025–12033; i) J. Elm, J. Lykkebo, T. J. Sørensen, B. W. Laursen, K. V. Mikkelsen, *J. Phys. Chem. A* **2012**, *116*, 8744–8752.

[17] O. Kel, P. Sherin, N. Mehanna, B. Laleu, J. Lacour, E. Vauthey, *Photochem. Photobiol. Sci.* **2012**, *11*, 623–631.

[18] A. Fürstenberg, O. Kel, J. Gradišar, T. R. Ward, D. Emery, G. Bollot, J. Mareda, E. Vauthey, *ChemPhysChem* **2009**, *10*, 1517–1532.

[19] a) A. Larsson, C. Carlsson, M. Jonsson, B. Albinsson, *J. Am. Chem. Soc.* **1994**, *116*, 8459–8465; b) J. T. Petty, J. A. Bordelon, M. E. Robertson, *J. Phys. Chem. B* **2000**, *104*, 7221–7227; c) A. Fürstenberg, T. G. Deligeorgiev, N. I. Gadjev, A. A. Vasilev, E. Vauthey, *Chem. Eur. J.* **2007**, *13*, 8600–8609.

[20] a) M. Kubista, B. Akerman, B. Norden, *Biochemistry* **1987**, *26*, 4545–4553; b) K. C. Hannah, B. A. Armitage, *Acc. Chem. Res.* **2004**, *37*, 845–853.

[21] C. Hiort, P. Lincoln, B. Norden, *J. Am. Chem. Soc.* **1993**, *115*, 3448–3454.

[22] E. Tuite, B. Norden, *J. Am. Chem. Soc.* **1994**, *116*, 7548–7556.

[23] K. Yamaoka, K. Matsuda, *Macromolecules* **1981**, *14*, 595–601.

[24] a) E. C. Long, J. K. Barton, *Acc. Chem. Res.* **1990**, *23*, 271–273; b) D. Suh, J. B. Chaires, *Bioorg. Med. Chem.* **1995**, *3*, 723–728.

[25] J. D. McGhee, P. H. Von Hippel, *J. Mol. Biol.* **1974**, *86*, 469–489.

[26] a) R. Xu, S. Dwarakanath, M. Cosman, S. Amin, N. E. Geacintov, *Carcinogenesis* **1996**, *17*, 2035–2042; b) I. Meistermann, V. Moreno, M. J. Prieto, E. Moldrheim, E. Sletten, S. Khalid, P. M. Rodger, J. C. Peberdy, C. J. Isaac, A. Rodger, M. J. Hannon, *Proc. Natl. Acad. Sci. USA* **2002**, *99*, 5069–5074; c) J. Malina, M. J. Hannon, V. Brabec, *Nucleic Acids Res.* **2008**, *36*, 3630–3638.

[27] A. R. Al Rabaa, F. Tfibel, F. Merola, P. Pernot, M. P. Fontaine-Aupart, *J. Chem. Soc. Perkin Trans. 2* **1999**, 341–351.

[28] B. W. Laursen, F. C. Krebs, *Chem. Eur. J.* **2001**, *7*, 1773–1783.

[29] R. Sens, K. H. Drexhage, *J. Lumin.* **1981**, *24*–*25*, 709–712.

[30] A. Wada, S. Kozawa, *J. Polym. Sci., Part A* **1964**, *2*, 853–864.

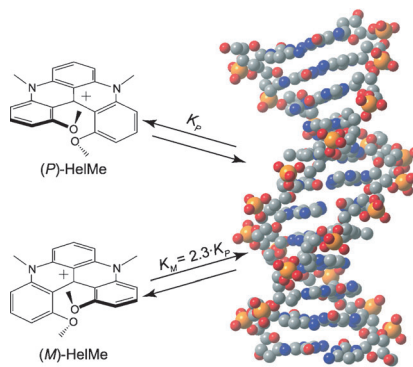
[31] B. Norden, M. Kubista, T. Kurucsev, *Q. Rev. Biophys.* **1992**, *25*, 51–170.

[32] P.-A. Muller, C. Högemann, X. Allonas, P. Jacques, E. Vauthey, *Chem. Phys. Lett.* **2000**, *326*, 321–327.

[33] a) A. Morandeira, L. Engeli, E. Vauthey, *J. Phys. Chem. A* **2002**, *106*, 4833–4837; b) G. Duvanel, J. Grilj, H. Chaumeil, P. Jacques, E. Vauthey, *Photochem. Photobiol. Sci.* **2010**, *9*, 908–915.

Received: November 1, 2012
Published online: ■■■, 0000

Getting in the groove! Chiral selectivity toward DNA binding is observed with fluorescent cationic helicene derivatives (see scheme). The binding to double-stranded DNA is evidenced by absorption, linear and circular dichroism spectroscopies, as well as stationary and time-resolved emission. A fluorescence enhancement of up to 4.4 is found in the presence of DNA. The binding constant to DNA, most probably through intercalation, is in all cases larger for the *M* than for the *P* enantiomer by factors ranging from 1.2 to 2.3.



DNA Probes

O. Kel, A. Fürstenberg, N. Mehanna, C. Nicolas, B. Laleu, M. Hammanson, B. Albinsson, J. Lacour, E. Vauthey* 

Chiral Selectivity in the Binding of [4]Helicene Derivatives to Double-Stranded DNA

